Food Chemistry: X 21 (2024) 101175

Contents lists available at ScienceDirect

Food Chemistry: X

journal homepage: www.sciencedirect.com/journal/food-chemistry-x

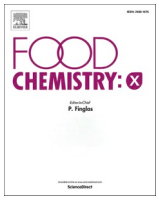

Metabolomic analysis to unravel the composition and dynamic variations of anthocyanins in bayberry-soaked wine during the maceration process

Yi Li [a,b], Shuangyang Chen [a,b], Xiamin Lyu [a], Xiugui Fang [a], Xuedan Cao [a,b,*]

[a] Zhejiang Citrus Research Institute, Taizhou, Zhejiang, China
[b] Key Laboratory of Fruit and Vegetable Function and Health Research of Taizhou, Zhejiang, China

ARTICLE INFO

Keywords:
Bayberry wine
Untargeted metabolomics
Anthocyanins
Maceration period

ABSTRACT

In this work, we employed a global untargeted metabolomics technique to explore the intricate composition of anthocyanin constituents in bayberry wine and elucidate their alteration during the maceration process. Our analysis uncovered 20 distinct forms of anthocyanins in bayberry wine, including cyanidin-type, delphinidin-type, peonidin-type, malvidin-type, and other-type. 'Dongkui' (DK) bayberry wine was characterized by a predominance of glycoside forms of cyanidin-type and delphinidin-type anthocyanins, while 'Shuijing' (SJ) bayberry wine mainly contained other-type anthocyanins. Additionally, differential anthocyanins analyses conducted across various maceration periods demonstrated the different fate of the components in the wine, with a conspicuous decline in most glycosidic form anthocyanins. Moreover, correlation analysis revealed that the red hue of bayberry wine was primarily associated with cyanidin-3-O-glucoside, cyanidin-3-O-rhamnoside, delphinidin-3-O-arabinoside, and delphinidin-3-O-galactoside. This research contributes to our understanding of the anthocyanin composition and the dynamic variations in bayberry wine, opening avenues for further exploration and optimization of production techniques in the future.

1. Introduction

Chinese bayberry (*Myrica rubra* Sieb. et Zucc.) is an edible fruit native to East Asia with popularity for its attractive color and delicious taste, and is also highly valued for its nutritional and medicinal properties (Ren et al., 2021; Sun et al., 2013; Zhang et al., 2022a). Modern pharmacological studies have proved that bayberry extracts possess multiple biological activities, including antioxidant, anti-inflammatory, anti-diabetic, and anti-cancer effects owing to the presence of various bioactive compounds like vitamins, flavonoids and phenolic acids (Ju et al., 2018; Liu et al., 2020; Lyu et al., 2021; Tu et al., 2022; Zhang et al., 2022a). Due to the extreme perishability of the fresh fruit, the harvested bayberries are often used for processing, in addition to fresh consumption. Among them, bayberry wine, a processed product formed by means of alcoholic maceration or yeast fermentation, has a long tradition in China as a medical wine for the treatment of diarrhea (Sarkar et al., 2022). However, color-presenting substances such as anthocyanins in bayberry wine usually show a series of changes during storage, which can seriously affect the appearance and merchantability of the product (Zhang et al., 2019). To improve the quality of bayberry wine, understanding the composition and changes of coloring substances is of great importance, yet current studies on the anthocyanin occurring in bayberry wine are very limited.

Anthocyanidin is the aglycones of anthocyanins, which can be divided into six basic categories according to the number of methoxyl and hydroxyl substituents on the B ring, including cyanidin (Cy), delphinidin (Dp), malvidin (Mv), pelargonidin (Pg), peonidin (Pn) and petunidin (Pt) (Xing et al., 2023). Naturally occurring anthocyanins are almost exclusively in the form of glycosides, containing sugar moieties like glucose, rhamnose, galactose, xylose or arabinose (Zang et al., 2022). Due to the different binding combinations between the aglycones and sugar moieties result in a wide variety of anthocyanins. To date, several anthocyanins have been reported in bayberry fruits. For instance, Fang et al. (2020) has reported cyanidin-3-O-glucoside was the major anthocyanin in bayberry fruits, while Lyu et al. (2021) has further identified seven different anthocyanins in the fruits like cyanidin-acetylapiosyl-glucoside, catechin-cyanidin-3-O-glucoside, delphinidin-3-O-glucoside and peonidin-3-O-glucoside, etc. However, comprehensive reports on anthocyanin profiles in bayberry wine remain scarce, with only handful of studies examining the alterations in total anthocyanins or the primary anthocyanins throughout the storage of the wine (Z. Zhang et al., 2019; Zhu et al., 2022). In addition, 'Dongkui' (DK) and

* Corresponding author at: Zhejiang Citrus Research Institute, Taizhou, Zhejiang, China.
E-mail address: xuedancao@outlook.com (X. Cao).

https://doi.org/10.1016/j.fochx.2024.101175
Received 3 August 2023; Received in revised form 21 January 2024; Accepted 1 February 2024
Available online 6 February 2024

'Shuijing' (SJ) are two representative cultivars of the bayberry, and 'SJ' bayberry fruit shows unique color of white or pinkish-white due to the reduced expression of key anthocyanin biosynthetic genes at the late stage of fruits development (Shi et al., 2018). Interestingly, our pre-experiments showed that the color of 'DK' bayberry wine gradually weaken in red hue during maceration, while that of 'SJ' bayberry wine gradually deepened from colorless, and eventually both wines presented a slightly yellow appearance. As mentioned above, these changes in color presentation are possible to be correlated with the anthocyanins involved and a further analysis is required.

To address this issue, we employed a global untargeted anthocyanin analysis technique to investigate the anthocyanin profiles and their abundance in bayberry wine at different maceration stages. Especially, we further compared the variations of anthocyanins in 'DK' and 'SJ' bayberry wine. Our study aims to facilitate a comprehensive understanding of the anthocyanin composition in different bayberry wines and the dynamics of anthocyanins during the maceration process, and provide theoretical basis for improving the merchantability of bayberry-soaked wine.

2. Materials and methods

2.1. Chemicals and materials

LC-MS grade methanol (MeOH) was purchased from Fisher Scientific (Loughborough, UK). Hydrochloric acid was obtained from Hushi (Shanghai, China). Ultrapure water was generated using a Milli-Q system (Millipore, Bedford, USA). All other chemicals and reagents used were of analytical grade unless otherwise noted.

2.2. Wine samples preparation and color analysis

Bayberry fruits of the cultivar 'Dongkui' and 'Shuijing' were harvested at commercial maturity in June 2022 from Taizhou city in Zhejiang province, China. The freshly picked fruits of uniform size with no mechanical damage and lesions were selected and washed for use. Bayberry wine is manufactured through the process of soaking the fruits in Chinese liquor (Baijiu) as the foundational base, creating a harmonious fusion of flavors during three months. Generally speaking, in a glass bottle with a lid, 300 g of cleaned bayberry fruit and 400 mL ''Zaoshao Baijiu'' (alcohol degree 52 % vol.) (Ningxi Zaoshao Baijiu Industry Co., Taizhou, China) were added, ensuring the fruits to be completely submerged. Then the samples were kept at 25±2 °C for 90 days. Three replicates were performed for each group. To be detected, 2 mL wine sample of each replicate was collected at 10th, 30th and 90th day, respectively. For convenience, samples of 'Dongkui' bayberry wine were named 'DK10′, 'DK30′ and 'DK90′, respectively. Accordingly, the wine samples of 'Shuijing' were marked as 'SJ 10′, 'SJ 30′ and 'SJ 90′, respectively.

Color parameters of the samples (L^*, a^*, b^*, C_{ab}^*, h_{ab}^*) were determined according to X. Zhang et al., (Zhang et al., 2021). For analysis, 2 mL of wine was passed through polyethersulfone filters to remove any impurities. Subsequently, the filtered wine was measured using a glass cuvette with a path length of 2 mm, while distilled water served as the reference. The visible absorption spectra (400–700 nm) of the wine were recorded using a UV–vis spectrophotometer (SP-756P, Shanghai spectrum instrument, China) at 1 nm intervals. The obtained data was then converted to CIE coordinates using the 10° Standard Observer and Standard Illuminant D65, as per the recommendations of the Commission International de L'Eclariage (CIE, 2004).

2.3. Anthocyanins analysis using untargeted techniques

All wine samples were stored at −20 °C prior to analysis. Then 100 μL of the sample was accurately transferred into a 2 mL centrifuge tube and vortexed for 60 s. Afterwards, the sample was centrifuged at 12,000 rpm and 4 °C for 10 min. The supernatant was then filtered through a 0.22 μm PTFE microporous membrane filters and transferred to the vial for LC-MS detection. Quality control (QC) samples were available by mixing all samples to form a pooled sample. All experiments were performed in triplicates.

A Vanquish UHPLC System (Thermo Fisher Scientific, USA) coupled to an Q-Exactive mass spectrometer equipped with ESI ion source (Thermo Fisher Scientific, USA) was used to analyze the global anthocyanin profiles. Chromatography was carried out with an ACQUITY UPLC BEH C_{18} (2.1 mm × 100 mm, 1.7 μm) (Waters, Milford, MA, USA) and the column temperature was maintained at 50 ℃. The flow rate and injection volume were set at 0.25 mL/min and 2 μL, respectively. For LC-ESI (+) MS analysis, the mobile phases consisted of (A) 1 % formic acid in water (v/v) and (B) 1 % formic acid in methanol (v/v). Separation was conducted under the following gradient: 0.0–2.0 min, 5 % B; 2.0–15.0 min, 5 %–70 % B; 15.0–15.1 min, 70 %−95 % B; 15.1–18.0 min, 95 % B; 18.0–20.0 min, 95 %−5% B; 20.0–25.0 min, 5 % B.

The primary and secondary mass spectrometry data (MS and MS/MS) were acquired using the following mass spectrometry conditions: sheath gas pressure, 47 arb; auxgas flow, 15 arb; spray voltage, 3.50 kV for ESI (+); capillary temperature, 320 ℃; MS range, 150–1300 *m/z*; MS resolving power, 70,000 FWHM; number of data dependent scans per cycle, 4; MS/MS resolving power, 17,500 FWHM; normalized collision energy, 10 eV, 50 eV, 60 eV.

2.4. Data processing

The raw data were firstly converted to mzML format by MSConvert in ProteoWizard software package (v3.0.8789) and processed using XCMS package (v3.20.0) in R software for feature detection, retention time correction and alignment. The robust SVR signal correction (QC-SVRC) was applied for data normalization to correct for any systematic bias. After normalization, only ion peaks with relative standard deviations (RSDs) less than 30 % in QC were kept to ensure proper metabolite identification. Afterwards, a three-dimension data sets containing *m/z*, peak retention time (RT) and peak intensities was exported to an Excel file, and subsequent analysis were performed on this basis.

2.5. Statistical analysis

The anthocyanins were identified by accuracy MS and MS/MS data which were matched with public databases including KNApSAcK (https://metabolomics.jp), HMDB (https://hmdb.ca), LipidMaps (https://lipidmaps.org), PubChem (https://pubchem.ncbi.nlm.nih.gov) and KEGG (https://www.genome.jp). Following qualitative analysis, the 'ropls' package (v1.30.0) in R software was used for multivariate data analysis and modelings. Hierarchical clustering analysis (HCA) dendrograms were constructed to analyze and visualize the diversity in metabolite profiles in different experimental groups. Principal component analysis (PCA) and (orthogonal) partial least-squares-discriminant analysis (O)PLS-DA were used to visualize the variations of anthocyanins among different groups. In addition, fold change (FC), variable influence on projection (VIP) values, and *p* values were applied to discover the differential anthocyanins.

3. Results and discussion

3.1. Anthocyanin profiles in bayberry wine

As shown in Fig. 1A, the bayberry wine underwent obvious color changes during different maceration periods, and the substances responsible for the color changes were reported to be mainly phenolic compounds, particularly anthocyanins from the fruit (Zhang et al., 2021). Therefore, we employed a global untargeted anthocyanin detection based on UHPLC-ESI-MS/MS analytical technique to identify the anthocyanins in bayberry wine during maceration. We divided the

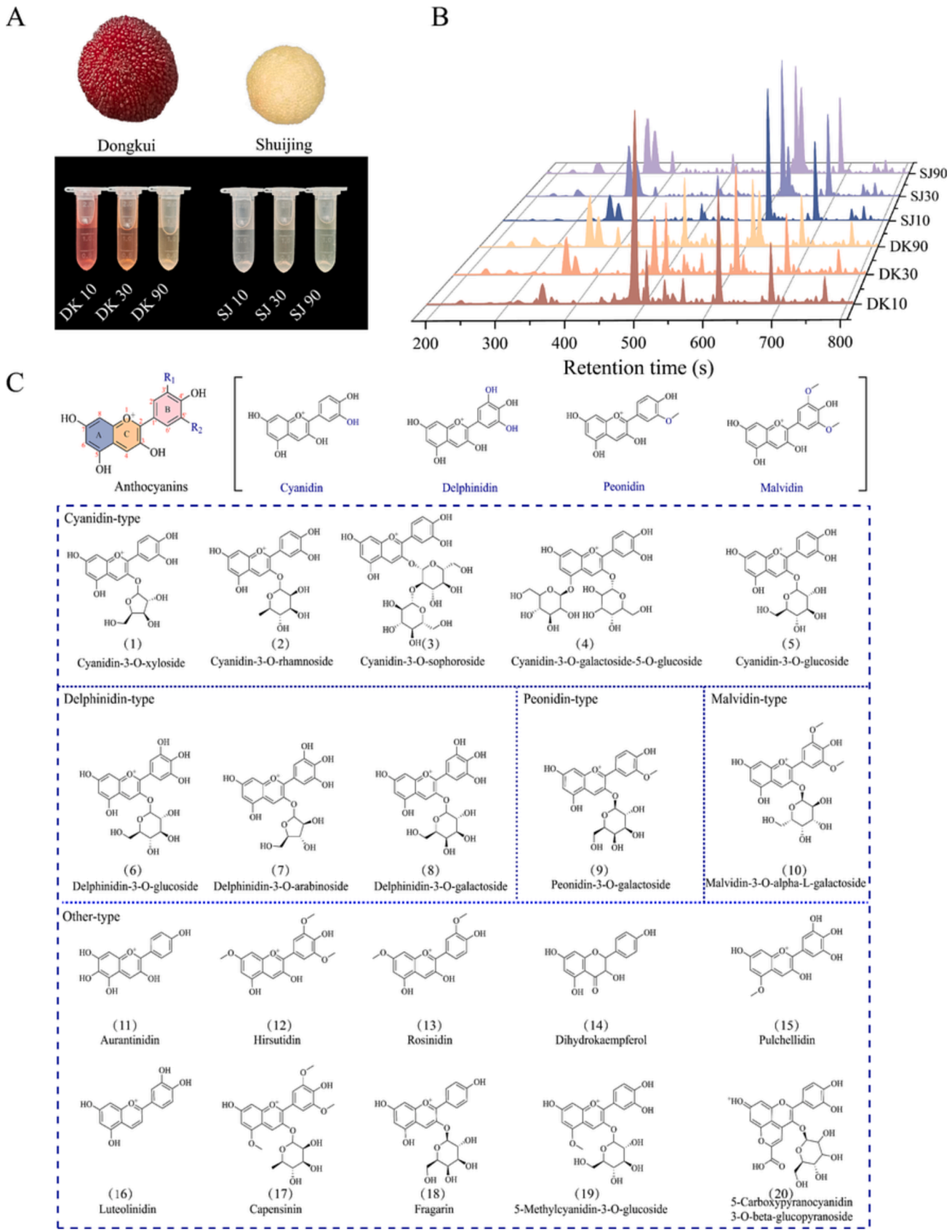

Fig. 1. Overall analysis of anthocyanin profiles in two kinds of bayberry wine. (A) Photographs of the fruit materials and bayberry wines. (B) Base peak chromatograms (BPC) of two bayberry wine samples at different maceration periods. (C) Structure of anthocyanins identified in bayberry wine by MS and MS/MS. Where 'DK10′, 'DK30′ and 'DK90′ represent 'Dongkui' bayberry wine samples collected at 10th, 30th and 90th day, respectively. Accordingly, 'SJ 10′, 'SJ 30′ and 'SJ 90′ refer to the samples of 'Shuijing' bayberry wine.

maceration period into three stages based on the color change of bayberry wine that could be observed with the naked eye, including the early maceration period (days 10–30), the late maceration period (days 30–90) and the whole maceration process (days 10–90). Fig. 1B represents the detected base peak chromatograms (BPC) of these two bayberry wines at different time points, showing the maximum intensity of each spectrum versus time in positive mode. Upon this, the difference of the peaks intensity in the two bayberry wine at specific retention times can be clearly observed.

A total of 20 anthocyanins were identified in the two bayberry wines, including four basic anthocyanins (Cy-type, Dp-type, Pn-type and Mv-type) as well as other-type anthocyanins (Fig. 1C). As shown, the Cy-type was the major anthocyanins in bayberry wine, which includes five different compounds. The Cy-type is one of the most abundant classes of anthocyanins in nature, especially in red berries such as blueberries, bayberries, mulberries, sweet cherries, and black chokeberries (Avula et al., 2023; Clodoveo et al., 2023). In our study, most of the monoglycosidic anthocyanins are substituted at the C-3 position, which is the common substituted form of anthocyanins. As reported, flavonoid 3-O-glycosyltransferases are the most widely distributed glycosyltransferases in plants, which is a key factor contributing to the prevalence of the 3-O-substituted form of anthocyanins (Yang et al., 2018). Commonly, cyanidin-3-O-glucoside (C3G) stands out as a major anthocyanin, prominently featured in a multitude of berry fruits (Avula et al., 2023). Herein, C3G was also the main anthocyanin presented in red 'DK' bayberry wine, which is consistent with what Zhang et al. (2020) have reported.

Lyu et al. (2021) had reported that the anthocyanins present in bayberry fruit were primarily identified as monoglycoside forms, while our investigation unveiled cyanidin-3-O-galactoside-5-O-glucoside, a diglycoside form anthocyanin, presenting in bayberry wine. Furthermore, peonidin-3-O-galactoside and malvidin-3-O-alpha-L-galactoside have been discovered in bayberry wine with a relative low level. Notably, malvidin-type has scarcely been reported in bayberry fruit and its derivative products before. In addition, other-type anthocyanins encompass six non-glycoside forms and four glycoside forms, which undergo structural modifications in the anthocyanidin skeletons. Notably, 5-Carboxypyranocyanidin-3-O-beta-glucopyranoside is a pyranoanthocyanin detected in the bayberry wine after being macerated for 10 days. Pyranoanthocyanins have been extensively reported as the predominant chromogenic substances in matured wines, such as 5-carboxypyranomalvidin-3-O-glucoside (vitisin A) (Zhang et al., 2022b), and this study also reveals the presence of vitisin-like pigments in bayberry wines.

3.2. Hierarchical clustering analysis

The variation of anthocyanin derivatives is visualized in the clustered heatmap shown in Fig. 2A. Hierarchical clustering reveals the presence of four distinct clusters, each characterized by unique component features. Generally, the components in cluster I showed a lower abundance in 'DK' bayberry wine compared to 'SJ' and tend to decrease over the maceration time. On the other hand, cluster II and III displayed a higher abundance of pigments in 'DK' bayberry wine against to 'SJ', with the notable difference being that the abundance of the compounds in cluster II tended to decrease with maceration time, while cluster III maintains a relatively stable level throughout the process. Lastly, cluster IV consists of substances initially present in low abundance and gradually increase over the maceration period.

The relevant components in cluster II and cluster III include cyanidin-3-O-glucoside, cyanidin-3-O-xyloside, cyanidin-3-O-rhamnoside, delphinidin-3-O-galactoside and delphinidin-3-O-glucoside, etc. As reported, cyanidin-type and delphinidin-type anthocyanins exhibit a captivating red or violet hue at a low pH (Zang et al., 2022). Accordingly, the apparently red color in 'DK' bayberry wine can be attributed to the presence of these pivotal pigments in cluster II and cluster III. In stark contrast, the intensity of these anthocyanins manifested markedly lower levels in the 'SJ' bayberry wine, which potentially accounts for its feeble coloration. Moreover, rosinidin, capensinin, and pulchellidin are A-ring methylated anthocyanin derivatives, however, the variation in their abundance may not contribute much to the color of the wine, as they make up a relatively low proportion of the pigments. In cluster IV, compounds such as fragarin, aurantindin and luteolinidin have a gradual rise in their intensity. Fragarin is a variant bounded with hydroxyl at C-1 position of pelargonidin-3-O-galactoside, presenting an orange color characteristic (Seeram et al., 2002). Aurantindin and luteolinidin are free anthocyanins and unstable in wine and may transfer to the reversed chalcones forms which can offer some pale yellow color (He et al., 2012). Thus, the color variation in the late stage bayberry wine is likely to be related to the increased abundance of the substances in cluster IV.

3.3. Anthocyanins variation analysis with pie charts

The anthocyanins in bayberry wine were categorized into five groups as illustrated by the pie charts (Fig. 2B). The primary anthocyanins found in the 'DK' bayberry wine predominantly belonged to the cyanidin-type, constituting approximately eighty percent of the total compounds, which is generally consistent with the anthocyanins reported in the literature for 'DK' bayberry fruits (Lin et al., 2019). In contrast, the 'SJ' bayberry wine contains a higher proportion anthocyanins belonging to other-type, and the proportion of basic type anthocyanins such as cyanidin, delphinidin, and peonidin derivatives is relatively low. Also, we found the evolution of anthocyanins in the two bayberry wines exhibited markedly distinct patterns with maceration time. In the case of 'DK', there was a slight upsurge in the total anthocyanin content from day 10 to day 30, followed by a notable decline from day 30 to day 90. Conversely, the abundance of anthocyanins in 'SJ' bayberry wine displayed a consistent tendency to increase as maceration progressed, accompanied by a gradual transition towards a yellow hue in the wine.

As know, anthocyanins are phenolic compounds that are most abundant in the cell vacuoles of the epidermis and subcutaneous tissues (Zhao et al., 2021). With the maceration technique, the dissolution of anthocyanins from the fruit necessitates the traversing of cellular barriers (Wojdyło et al., 2021). Despite the uniformity of conditions (alcohol concentration, temperature, and time), the composition of anthocyanins within the two varieties diverse markedly, thereby exhibiting different evolutionary patterns as maceration progresses. These may be the primary factors responsible for the divergent trends observed in the anthocyanin abundance within the two bayberry wines.

3.4. PCA and PLS-DA analysis

By using the heatmap, metabolites participating in different maceration periods of bayberry wines can be easily distinguished. In order to improve data interpretability, we applied multivariate statistical analysis techniques including PCA and PLS-DA models to reduce the dimensionality of the metabolites. Firstly, we run an unsupervised PCA model on bayberry wine samples from different maceration periods, which can effectively reflect the overall inter- and intra-group variability and reflect the distribution trends in different samples. PCA score plot that composed of the first and second principal components (PC1 and PC2) was shown in Fig. 3A; sample score values clearly showed the variations among different groups. The PC1 effectively separated the 'DK' and 'SJ' bayberry wines, with 'SJ' and 'DK' scores mainly located on the positive and negative axis of PC1, respectively. Furthermore, as the maceration time progresses from 10 days to 30 days and 90 days, both of 'DK' and 'SJ' points gradually shift from the positive axis to the negative axis of the PC2. The above results indicate that the PC1 mainly reflects the differences in anthocyanin components in the two types of bayberry wine, and the PC2 represents the evolutionary pattern of

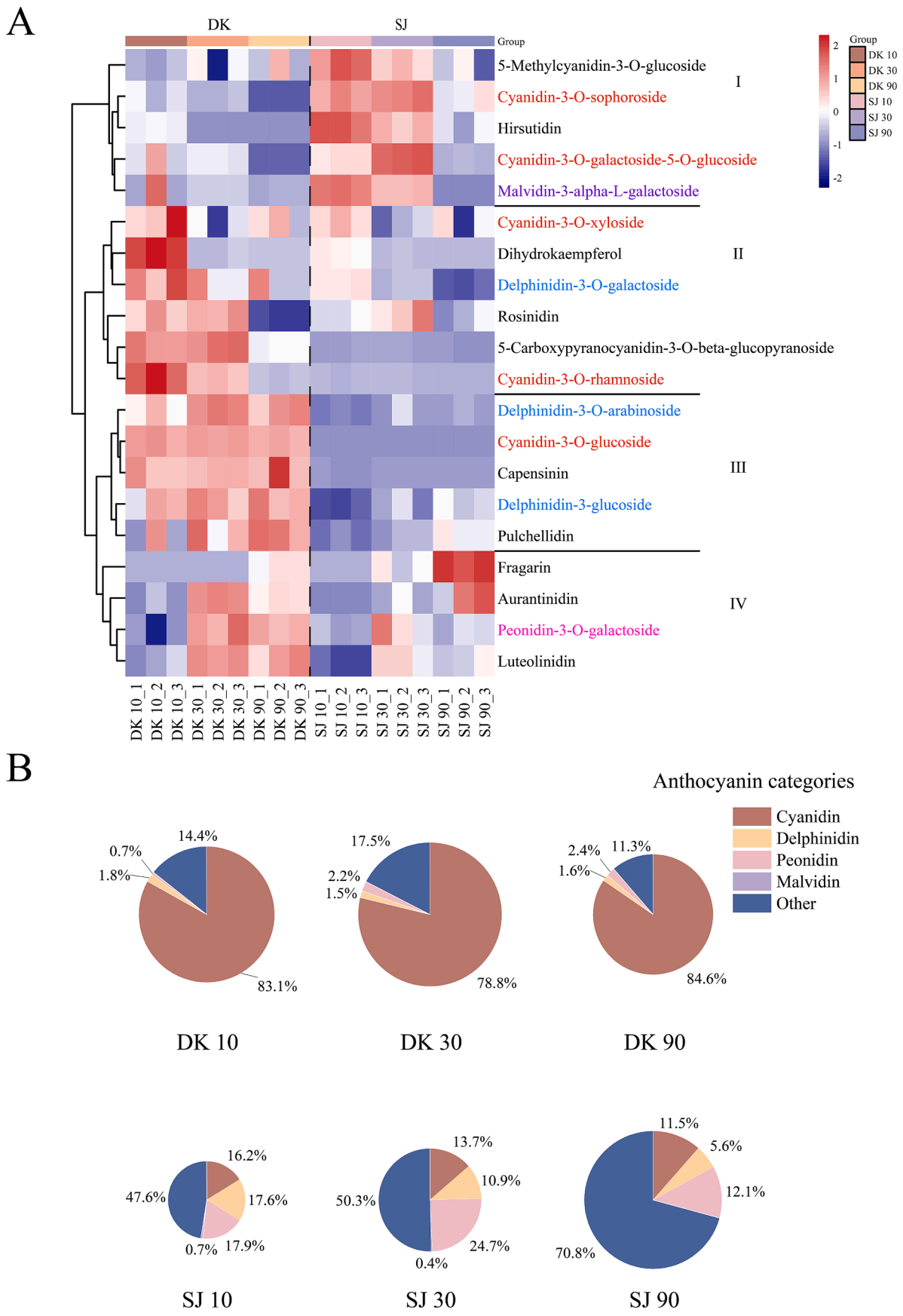

Fig. 2. Anthocyanins variation analysis with hierarchical clustering and pie charts. (A) Clustered heatmap showing the difference of anthocyanins in different groups. (B) Pie charts depicting the variation of the five categories of anthocyanins among different groups.

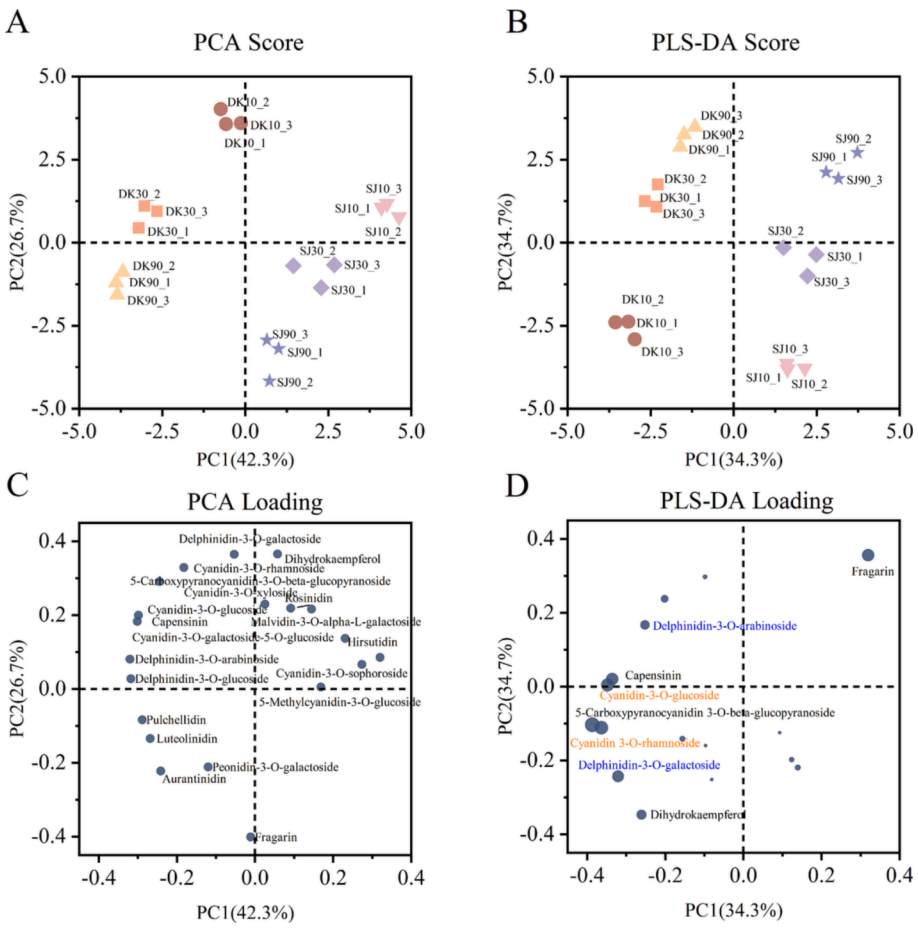

Fig. 3. Principal component analysis (PCA) and partial least-squares-discriminant analysis (PLS-DA). (A) PCA score plot. (B) PLS-DA score plot. (C) PCA loading plot. (D) PLS-DA loading plot, where the size of the scatter represents the VIP value calculated by this model.

anthocyanins during the maceration process.

Combined with the PCA loading plot (Fig. 3C), the anthocyanins of cyanidin-type and delphinidin-type on the negative x-axis are the characteristic components of 'DK' bayberry wine, while hirsutidin, cyanidin-3-O-sophoroside, and 5-methycyanidin-3-O-glucoside on the positive x-axis are characteristic anthocyanins of 'SJ' bayberry wine. In addition, pulchellidin, luteolinidin, fragarin, and aurantinidin may be the characteristic substances that mainly changed during maceration. Two primary factors contribute to the discrepancies in characteristic anthocyanins in different samples. The first factor concerns the variances in anthocyanin fractions and concentrations present in 'DK' and 'SJ' fruits, as noted by Lyu et al. (2021). The second factor is owing to the differences in anthocyanin leaching and alterations during the prolonged maceration process (Wojdyło et al., 2021).

Unsupervised PCA analysis does not facilitate the detection of between-group differences and differential compounds by ignoring within-group errors and eliminating random errors that are not relevant to the purpose of the study. To further focus on the point of interest, the data needs to be analyzed using prior knowledge of the sample with supervised pattern recognition methods. Partial least squares-discriminate analysis (PLS-DA) is currently the most commonly used classification method in the analysis of metabolomics data, which combines a regression model with dimensionality reduction and uses certain discriminant thresholds for discriminant analysis of regression results to efficiently extract information on inter-group variation.

In this study, the results of the discriminant analysis using PLS-DA are shown in Fig. 3B, where the differences between the samples are clearly marked. PC1 and PC2 together explained 69.0 % of the variation between groups. Compared to the PCA scores, PC1, which represents the difference in composition between the two types of bayberry wine, decreased slightly in the PLS-DA model, and PC2, which represents the variation with maceration time, increased slightly. The PLS-DA loading plot (Fig. 3D) shows the compounds that contributed significantly to these differences, where the size of the scatter represents the VIP value calculated by the model. We found that cyanidin-3-O-glucoside, cyanidin-3-O-rhamnoside (cyanidin-type), delphinidin-3-O-galactoside, delphinidin-3-O-arabinoside (delphindin-type), 5-carboxypyranocyanidin-3-O-beta-glucopyranoside, fragarin, capensinin and dihydrokaempferol were the main discriminant compounds contributing to the whole difference among groups.

3.5. *Analysis of differential markers*

At this point, we used the OPLS-DA model to screen the representative differential substances in the bayberry wine at different maceration periods.

3.5.1. *'DK' bayberry wine*

The results of the OPLS-DA comparison for the different groups of 'DK' bayberry wine are presented in Fig. 4. As can be seen, the OPLS-DA score plot Fig. 4(A – C) shows a high degree of differentiation between the groups of samples, with a clear separation of the different maceration periods for 'DK' bayberry wine. Furthermore, excellent model parameters were detected in our experiments (day 10 – day 30: R2Y = 0.991, Q2 = 0.956; day 30 – day 90: R2Y = 0.999, Q2 = 0.931; day 10 – day 90: R2Y = 0.995, Q2 = 0.969). In addition, the VIP value in the OPLS-DA analysis was considered a valid parameter for evaluating the strength and interpretability of the effect of the expression pattern

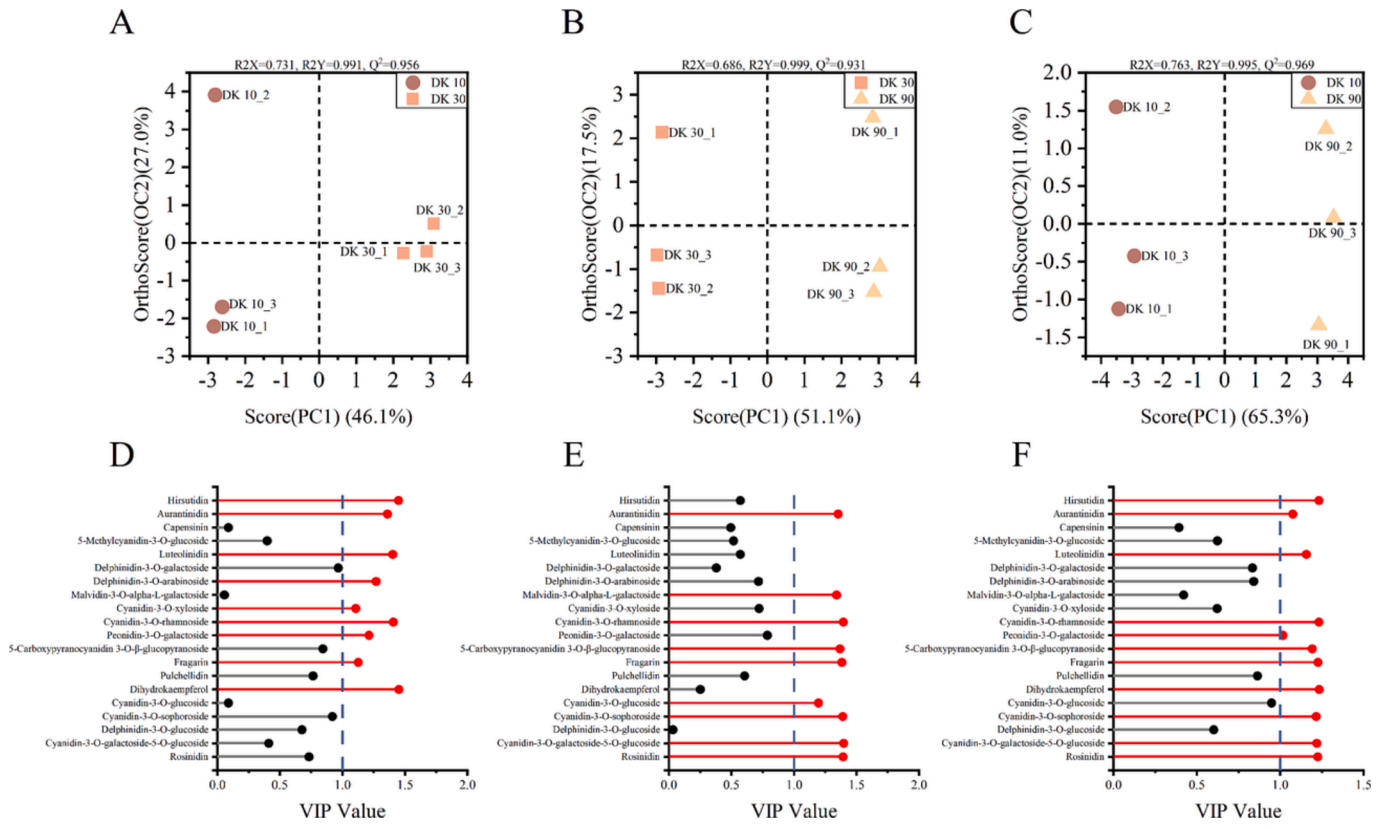

Fig. 4. Analysis of differential markers in 'DK' bayberry wine. (A–F) OPLS-DA score plots of samples during maceration periods and the corresponding VIP values (A, D: day 10 and day 30; B, E: day 30 and day 90; C, F: day 10 and day 90).

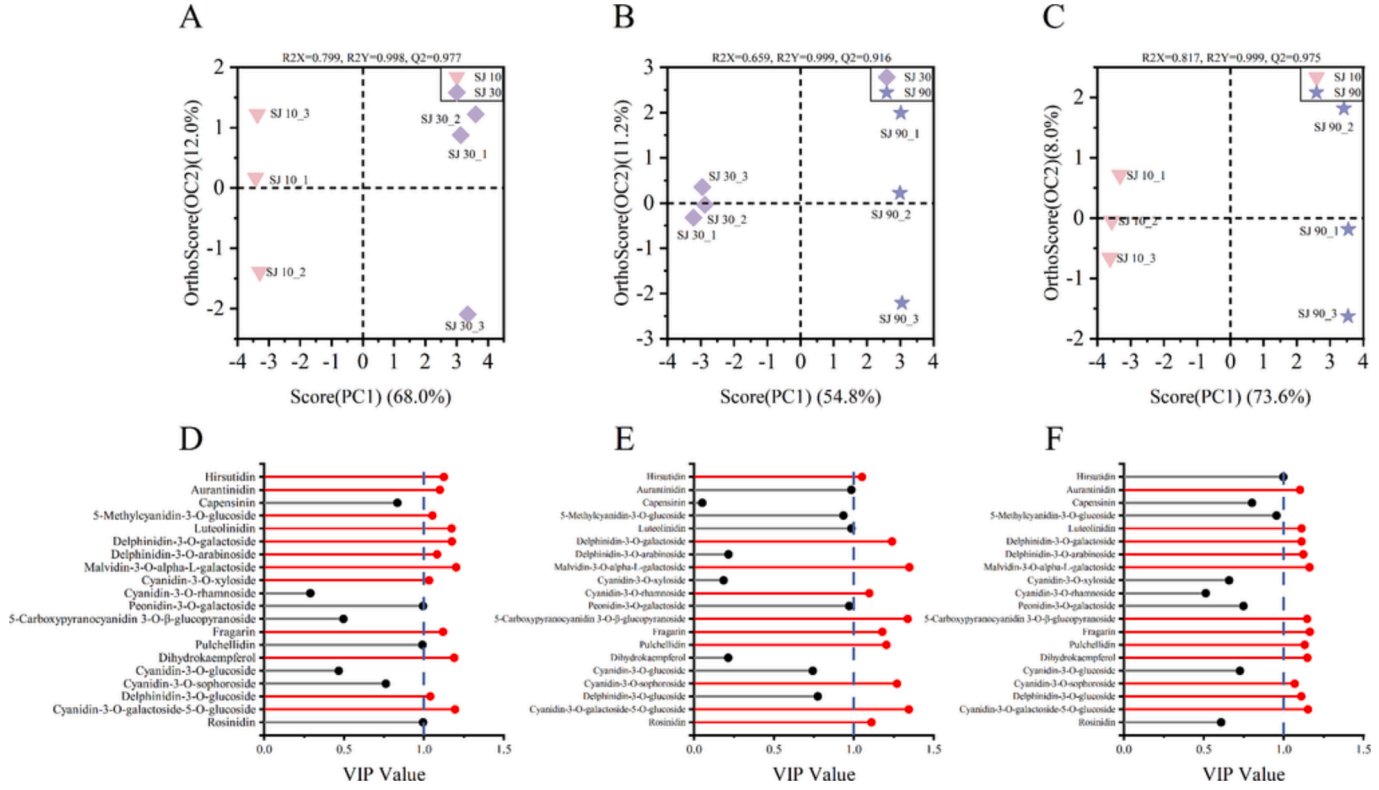

Fig. 5. Analysis of differential markers in 'SJ' bayberry wine. (A–F) OPLS-DA score plots of samples during maceration periods and the corresponding VIP values (A, D: day 10 and day 30; B, E: day 30 and day 90; C, F: day 10 and day 90).

between groups, and a higher VIP value indicated a greater contribution of the variable to the grouping. Usually metabolites with a VIP value >1.0 are considered as differential metabolites.

The VIP values for the comparison between different groups of 'DK' bayberry wine are shown in Fig. 4(D − E), where the horizontal coordinates indicate the magnitude of the VIP values, with VIP >1.0 as the cut-off. Aurantinidin, cyanidin-3-O-rhamnoside and fragarin are three components that are significant markers at all times, indicating that these substances underwent continuous and significant changes in abundance throughout the maceration process. Whereas hisutidin, luteolinidin, penidin-3-O-galacoside and dihydrokaempferol were significant differentials from day 10 to day 30, while they were not significant differentials from day 30 to day 90, suggesting that they changed mainly in the first stage of maceration. In contrast, 5-carboxypyranocyanidin-3-O-beta-glucopyranoside, cyanidin-3-O-sophoroside, cyanidin-3-O-galactoside-5-O-glucoside served as representative differentials only during day 30 to day 90, indicating their changes occurred mainly in the second stage. At last, capensinin, 5-methylcyanidin-3-O-glucoside, delphinidin-3-O-galactoside, pulchellidin and delphinidin-3-O-glucoside were not significant differentials among the whole maceration periods, suggesting that they are relatively stable during the maceration process.

3.5.2. 'SJ' bayberry wine

The results of the OPLS-DA comparison for the three groups of 'SJ' bayberry wines are shown in Fig. 5. It can be seen that, similarly to the 'DK' bayberry wine, the OPLS-DA score plot in Fig. 5(A − C) shows a clear separation of the SJ bayberry wines at different maceration times. In addition, the VIP values calculated based on the OPLS-DA model for the comparison between different groups of 'SJ' bayberry wines are shown in Fig. 5(D − F). Delphinidin-3-O-galactoside, malvidin-3-O-alpha-L-galactoside, fragarin and cyanidin-3-O-galactoside-5-O-glucoside were significant markers at all times, indicating that these substances underwent continuous changes in abundance throughout the maceration process. It is interesting to note that fragarin was a significant marker throughout the maceration process in both 'DK' and 'SJ' bayberry wines. In contrast, aurantinidin, luteolinidin, delphinidin-3-O-arabinoside, delphinidin 3-O-glucoside and dihydrokaempferol showed significant differences from 10d to 30d, while they did not show significant differences from 30d to 90d, suggesting they mainly changed during the first maceration stage. In addition, 5-carboxypyranocyanidin-3-O-beta-glucopyranoside, cyanidin-3-O-sophoroside, pulchellidin, cyanidin-3-O-rhamnoside and rosinidin only show representative differences from day 30 to day 90 of maceration, indicating their changes occurred mainly in the second phase. Moreover, capensinin, peonidin-3-O-galactoside and cyanidin-3-O-glucoside were not significant differentials during maceration periods, suggesting they are relatively stable in 'SJ' bayberry wine.

The study resulted in the screen of anthocyanin differentials in 'DK' and 'SJ' wines during maceration periods, and the analysis of their variation pattern. We observed distinct anthocyanin compounds suffered different variations, which may be related to their unique molecular architectures and inherent attributes (Zhang et al., 2022b). Compared to previous report (Z. Zhang et al., 2019), our study examined the changes in anthocyanin components in a more comprehensive manner, which provides further insights into the relationship between anthocyanin profiles and the coloring of bayberry wine.

3.5.3. Differential anthocyanin metabolites screened by fold change and VIP

Furthermore, the two bayberry wines were screened for differential anthocyanins at different times based on fold change (log2 (FC) >1), VIP values >1 and p-values < 0.05, and the results are shown in Table S1. Together, the bar chart in Fig. S1 presents the differential anthocyanin expression during maceration periods of the two varieties of bayberry wine. Overall, the proportion of the 20 anthocyanins identified in 'DK' bayberry wine that decreased in abundance was significantly greater than that increased. After 90 days of maceration, three anthocyanins significantly increased in abundance, including frigarin (30.034-fold), aurantinidin (3.733-fold) and peonidin-3-O-galactoside (3.179-fold), while six anthocyanins significantly decreased in abundance, including cyanidin-3-O-sophoroside (27.027-fold), cyanidin 3-O-galactoside-5-O-glucoside (23.256-fold), and cyanidin-3-O-rhamnoside (12.658-fold), etc. The decrease of the aforementioned anthocyanins occurred mainly in the period of 30d to 90d. In contrast, dihydrokaempferol and hirsutidin decreased to a lesser extent and occurred mainly in the first stage of maceration.

In our experiment, a discernible diminishment of the red hue was observed in 'DK' bayberry wine during maceration process, and the phenomenon is similar to the red hue diminishing in young red wines. The researchers have attributed this phenomenon to the decline of monomeric anthocyanins (Dipalmo et al., 2016). However, unraveling the intricate interplay between the anthocyanin reduction and the resultant chromatic appearance within a complex fruit wine system is quite difficult. It may be feasible to further explore the relationship by constructing a bayberry wine model, as reported by the Zhang et al. (Zhang et al., 2020), with a special focus on the differential anthocyanins that we have identified.

In 'SJ' bayberry wine, after 90 d of maceration, the greatest increase anthocyanin was fragarin (40.133-fold), followed by aurantinidin (13.033-fold), which is in agreement with 'DK' bayberry wine. Anthocyanin components that decreased in 'SJ' bayberry wine included malvidin-3-alpha-L-galactoside (19.608-fold), delphinidin-3-O-galactoside (8.197-fold), and dihydrokaempferol (2.618-fold). Their decrease occurred mainly during the maceration process from day 30 to day 90. Dihydrokaempferol and 5-carboxypyranocyanidin-3-O-beta-glucopyranoside were found to decrease significantly in both 'DK' and 'SJ' bayberry wine, indicating a consistency in their evolution during the maceration of two bayberry wines.

Throughout the process of maceration, the changes of anthocyanins within 'DK' and 'SJ' wine led to a conspicuous decline in most glycosidic form pigments. Notably, Muche et al. (2018) suggested that glycosidic hydrolysis was a major cause of anthocyanin degradation, which is similar with the results we detected. In addition to hydrolysis, oxidation emerges as another prominent reason for the diminution of anthocyanins within the wine. Because the adjacent hydroxyl groups of o-diaphanous are sensitive to oxidation (He et al., 2012), compounds such as cyanidin-type and delphinidin-type anthocyanins are more susceptible to oxidation, whereas compounds without this structure such as peonidin-type, fragarin, aurantinidin, and lueolindin exhibit more resistance against the oxidation.

3.6. Correlation analysis

The correlation between the color attributes and anthocyanin profiles of bayberry wine were revealed by calculating Pearson correlation coefficients, and the results were depicted in Fig. 6. L^* values (luminosity) showed a significant negative correlation with components like cyanidin-3-O-glucoside, dihydrokaempferol, carboxypyranocyanidin-3-O-beta-glucopyranoside, cyanidin-3-O-rhamnoside, delphinidin-3-O-arabinoside, delphinidin-3-O-galactoside, and capensinin. Commonly, the wine of deep color tends to exhibit a reduction of its brightness and transparency, while also show a decrease in L^* value (Zhang et al., 2022b). So the results indicated that the mentioned anthocyanins play a crucial role in enhancing the color depth of bayberry wine. In addition, in the case of the a^* values, these compounds exhibited a substantial positive correlation, underscoring their role in imparting the red hue. Moreover, it is noteworthy that the attenuation of red color was accompanied by a gradual decrease in the abundance of these compounds during the maceration process. Our findings align with the observations documented in many other fruit wines (X. Li et al., 2020; Schmitzer et al., 2010; Sun et al., 2019; Yuan et al., 2023).

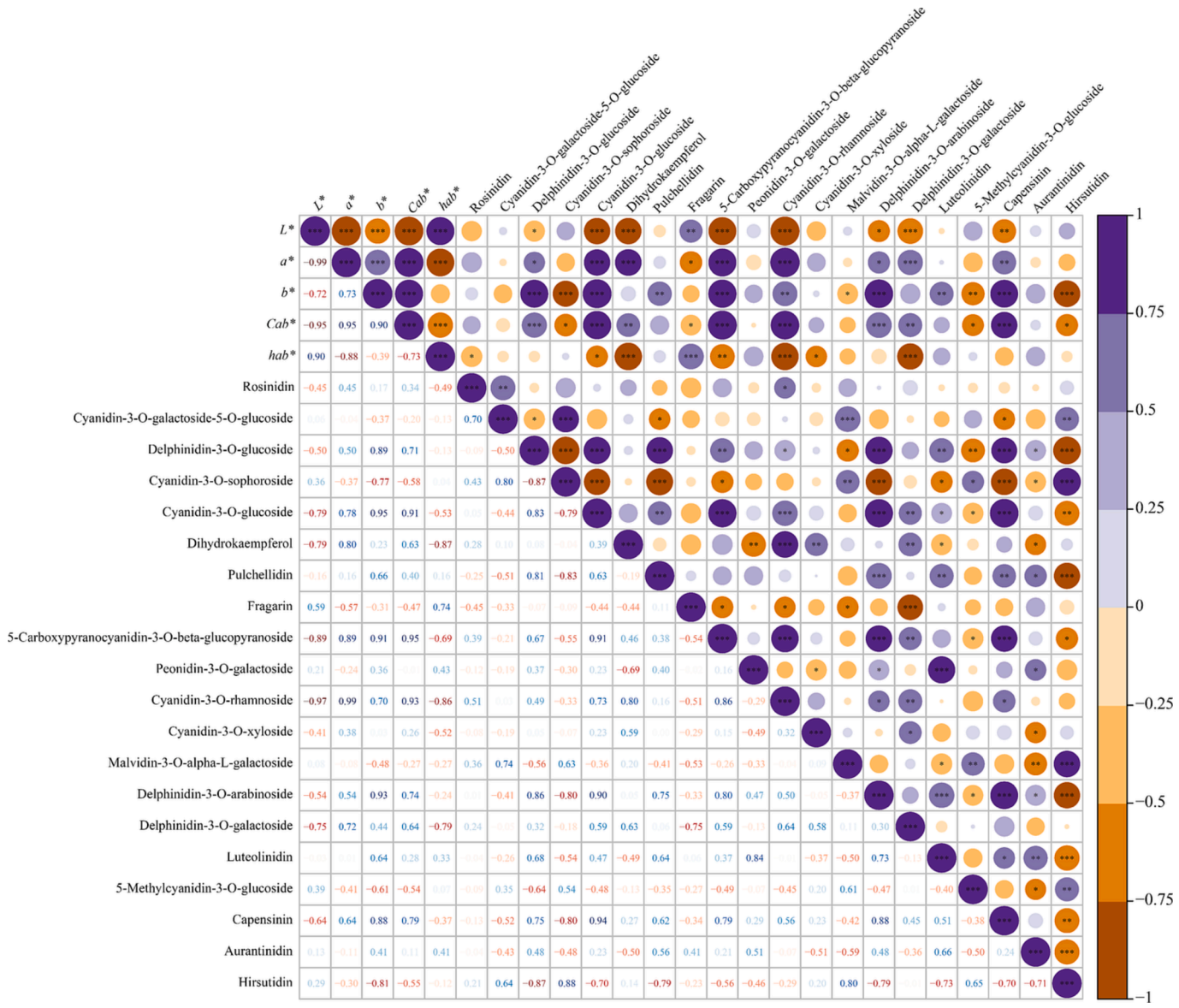

Fig. 6. Correlation heatmap depicting Pearson correlation coefficients between color attributes and anthocyanin profiles of bayberry wine.

For the b^* values, delphinidin-3-O-glucoside, cyanidin-3-O-glucoside, carboxypyranocyanidin-3-O-beta-glucopyranoside, delphinidin-3-O-arabinoside and capensinin exhibited a pronounced positive correlation, while cyanidin-3-O-sophoroside, methylcyanidin-3-O-glucoside, hirsutidin demonstrated significant negative correlations. In 'DK' bayberry wine, b^* values tended to initially increase followed by a subsequent decline with maceration, while b^* values of 'SJ' bayberry increased at the beginning and then kept stabilization (Fig. S2). Combined with the color appearance of bayberry wine in the late stage, it suggests that the components responsible for the yellow hue may be relatively stable, while the anthocyanins responsible for the red hue are unstable in the wine.

Furthermore, it is noteworthy that the anthocyanins linked to the a^* and b^* values exhibited a consistent correlation in C_{ab}^* (chroma). This can be attributed to the definition of C_{ab}^*, which is determined by the mathematical square root of the sum of the squares of the a^* and b^* values. During maceration, the C_{ab}^* values of 'DK' bayberry wine gradually decreased, while the C_{ab}^* values of 'SJ' bayberry wine increased and then stabilized (Fig. S2). The reduction in C_{ab}^* values has been documented in sweet wines (Figueiredo-González et al., 2014), and it was ascribed to the degradation of anthocyanins during the aging process or the formation of complex pigments, which aligns with the findings observed in 'DK' bayberry wine. In contrast, the correlation between h_{ab}^* (tonality) and anthocyanins was significantly different from a^*, b^* and C_{ab}^*, but more similar to L^* values, and the trend of both h_{ab}^* and L^* showed a gradual increase during the maceration of bayberry wines. In other wine storage and aging studies, the gradual increasing in h_{ab}^* and L^* has also been observed (Li et al., 2021; Zhang et al., 2021).

4. Conclusions

In summary, our comprehensive untargeted analysis of anthocyanins in bayberry wine revealed the presence of 20 distinct forms compounds, classified as cyanidin-type, delphinidin-type, peonidin-type, malvidin-type, and other-type anthocyanins. Notably, we report for the first time the identification of cyanidin-3-O-galactoside-5-O-glucoside, malvidin-3-O-alpha-L-galactoside, and 5-carboxypyranocyanidin-3-O-beta-glucopyranoside in bayberry wines. Furthermore, the variations in the proportions of anthocyanins between 'DK' and 'SJ' bayberry wines contribute to their distinct visual characteristics. Specifically, 'DK' wine exhibits a predominance of glycoside forms of cyanidin-type and

delphinidin-type anthocyanins, while 'SJ' wine primarily contains other-type anthocyanins. Analyses conducted on the alterations of anthocyanins profiles across various maceration periods revealed that different anthocyanins suffer distinct change fate in the wine. While, the variation trend of the same anthocyanin in 'DK' and 'SJ' wines was similar. In addition, correlation analysis revealed that the red hue presentation of the bayberry wine is primarily associated with the glycoside form of anthocyanins, such as cyanidin-3-O-glucoside, cyanidin-3-O-rhamnoside, delphinidin-3-O-arabinoside, and delphinidin-3-O-galactoside. Conversely, the non-glycoside form of anthocyanins exhibited a weak correlation with coloration. Moving forward, a targeted analysis focusing on the variations in key anthocyanins during maceration, as well as an exploration of the impact of processing techniques on these changes, will contribute to the development of effective strategies for regulating the color of bayberry wine.

CRediT authorship contribution statement

Yi Li: Investigation, Methodology, Software, Writing – original draft. **Shuangyang Chen:** Methodology, Writing – review & editing. **Xiamin Lyu:** Methodology, Software, Writing – review & editing. **Xiugui Fang:** Conceptualization, Writing – review & editing. **Xuedan Cao:** Conceptualization, Funding acquisition, Investigation, Supervision, Writing – review & editing.

Declaration of competing interest

The authors declare that they have no known competing financial interests or personal relationships that could have appeared to influence the work reported in this paper.

Data availability

Data will be made available on request.

Acknowledgements

We feel very grateful for the metabolites identification provided by Suzhou PANOMIX Biomedical Tech Co., Ltd. (Suzhou, China).

Appendix A. Supplementary data

Supplementary data to this article can be found online at https://doi.org/10.1016/j.fochx.2024.101175.

References

Avula B., Katragunta K., Osman A.G., Ali Z., John Adams S., Chittiboyina A.G., & Khan I. A. (2023). Advances in the chemistry, analysis and adulteration of anthocyanin rich-berries and fruits: 2000–2022. *Molecules*. *28*(2). Article 2. 10.3390/molecules28020560.

Clodoveo, M. L., Crupi, P., Muraglia, M., Naeem, M. Y., Tardugno, R., Limongelli, F., & Corbo, F. (2023). The main phenolic compounds responsible for the antioxidant capacity of sweet cherry (Prunus avium L.) pulp. *LWT, 185*, Article 115085. https://doi.org/10.1016/j.lwt.2023.115085

Dipalmo, T., Crupi, P., Pati, S., Clodoveo, M. L., & Di Luccia, A. (2016). Studying the evolution of anthocyanin-derived pigments in a typical red wine of Southern Italy to assess its resistance to aging. *LWT - Food Science and Technology, 71*, 1–9. https://doi.org/10.1016/j.lwt.2016.03.012

Fang, Z.-X., Zhang, M., Wang, L.-X., & Sun, J.-C. (2020). Identification of anthocyanin in bayberry (Myrica rubra Sieb. Et Zucc.) by HAPLC-DAD-ESIMS and GC. *Journal of Food and Drug Analysis, 14*(4). https://doi.org/10.38212/2224-6614.2457

Figueiredo-González, M., Cancho-Grande, B., Simal-Gándara, J., Teixeira, N., Mateus, N., & De Freitas, V. (2014). The phenolic chemistry and spectrochemistry of red sweet wine-making and oak-aging. *Food Chemistry, 152*, 522–530. https://doi.org/10.1016/j.foodchem.2013.12.018

He, F., Liang, N.-N., Mu, L., Pan, Q.-H., Wang, J., Reeves, M. J., & Duan, C.-Q. (2012). Anthocyanins and their variation in red wines I. Monomeric anthocyanins and their color expression. *Molecules, 17*(2), Article 2. https://doi.org/10.3390/molecules17021571

Ju, J., Yao, W., Sun, S., Guo, Y., Cheng, Y., Qian, H., & Xie, Y. (2018). Assessment of the antibacterial activity and the main bacteriostatic components from bayberry fruit extract. *International Journal of Food Properties, 21*(1), 1043–1051. https://doi.org/10.1080/10942912.2018.1479861

Li, M., Zhao, X., Sun, Y., Yang, Z., Han, G., & Yang, X. (2021). Evaluation of anthocyanin profile and color in sweet cherry wine: Effect of sinapic acid and grape tannins during aging. *Molecules, 26*(10), 2923. https://doi.org/10.3390/molecules26102923

Li, X., Zhang, L., Peng, Z., Zhao, Y., Wu, K., Zhou, N., Yan, Y., Ramaswamy, H. S., Sun, J., & Bai, W. (2020). The impact of ultrasonic treatment on blueberry wine anthocyanin color and its in-vitro anti-oxidant capacity. *Food Chemistry, 333*, Article 127455. https://doi.org/10.1016/j.foodchem.2020.127455

Lin, Q., Zhong, Q., & Zhang, Z. (2019). Comparative transcriptome analysis of genes involved in anthocyanin biosynthesis in the pink-white and red fruits of Chinese bayberry (Morella rubra). *Scientia Horticulturae, 250*, 278–286. https://doi.org/10.1016/j.scienta.2019.02.061

Liu, Y., Zhang, X., Zhan, L., Xu, C., Sun, L., Jiang, H., Sun, C., & Li, X. (2020). LC-Q-TOF-MS characterization of polyphenols from white bayberry fruit and its antidiabetic effect in KK-A ^{y} mice. *ACS Omega, 5*(28), 17839–17849. https://doi.org/10.1021/acsomega.0c02759

Lyu, Q., Wen, X., Liu, Y., Sun, C., Chen, K., Hsu, C.-C., & Li, X. (2021). Comprehensive profiling of phenolic compounds in white and red chinese bayberries (Morella rubra Sieb. Et Zucc.) and their developmental variations using tandem mass spectral molecular networking. *Journal of Agricultural and Food Chemistry, 69*(2), 741–749. https://doi.org/10.1021/acs.jafc.0c04117

Muche, B. M., Speers, R. A., & Rupasinghe, H. P. V. (2018). Storage temperature impacts on anthocyanins degradation, color changes and haze development in juice of "Merlot" and "Ruby" grapes (Vitis vinifera). *Frontiers in Nutrition, 5*. https://doi.org/10.3389/fnut.2018.00100

Ren, H., He, Y., Qi, X., Zheng, X., Zhang, S., Yu, Z., & Hu, F. (2021). The bayberry database: A multiomic database for *Myrica rubra*, an important fruit tree with medicinal value. *BMC Plant Biology, 21*(1), 452. https://doi.org/10.1186/s12870-021-03232-x

Sarkar, T., Salauddin, M., Roy, A., Sharma, N., Sharma, A., Yadav, S., Jha, V., Rebezov, M., Khayrullin, M., Thiruvengadam, M., Chung, I.-M., Shariati, M. A., & Simal-Gandara, J. (2022). Minor tropical fruits as a potential source of bioactive and functional foods. *Critical Reviews in Food Science and Nutrition*, 1–45. https://doi.org/10.1080/10408398.2022.2033953

Schmitzer, V., Veberic, R., Slatnar, A., & Stampar, F. (2010). Elderberry (Sambucus nigra L.) wine: A product rich in health promoting compounds. *Journal of Agricultural and Food Chemistry, 58*(18), 10143–10146. https://doi.org/10.1021/jf102083s

Seeram, N. P., Schutzki, R., Chandra, A., & Nair, M. G. (2002). Characterization, quantification, and bioactivities of anthocyanins in *Cornus* species. *Journal of Agricultural and Food Chemistry, 50*(9), 2519–2523. https://doi.org/10.1021/jf0115903

Shi, L., Chen, X., Chen, W., Zheng, Y., & Yang, Z. (2018). Comparative transcriptomic analysis of white and red Chinese bayberry (Myrica rubra) fruits reveals flavonoid biosynthesis regulation. *Scientia Horticulturae, 235*, 9–20. https://doi.org/10.1016/j.scienta.2018.02.076

Sun, C., Huang, H., Xu, C., Li, X., & Chen, K. (2013). Biological activities of extracts from Chinese bayberry (Myrica rubra Sieb. et Zucc.): A review. *Plant Foods for Human Nutrition, 68*(2), 97–106. https://doi.org/10.1007/s11130-013-0349-x

Sun, X., Yan, Z., zhu, T., Zhu, J., Wang, Y., Li, B., & Meng, X. (2019). Effects on the color, taste, and anthocyanins stability of blueberry wine by different contents of mannoprotein. *Food Chemistry, 279*, 63–69. https://doi.org/10.1016/j.foodchem.2018.11.139

Tu, P., Tang, Q., Wang, M., Chen, W., Ye, X., & Zheng, X. (2022). Protective role of bayberry extract: Associations with gut microbiota modulation and key metabolites. *Food & Function, 13*(10), 5547–5558. https://doi.org/10.1039/D1FO04253J

Wojdyło, A., Samoticha, J., & Chmielewska, J. (2021). Effect of different pre-treatment maceration techniques on the content of phenolic compounds and color of Dornfelder wines elaborated in cold climate. *Food Chemistry, 339*, Article 127888. https://doi.org/10.1016/j.foodchem.2020.127888

Xing, C., Chen, P., & Zhang, L. (2023). Computational insight into stability-enhanced systems of anthocyanin with protein/peptide. *Food Chemistry: Molecular Sciences, 6*, Article 100168. https://doi.org/10.1016/j.fochms.2023.100168

Yang, B., Liu, H., Yang, J., Gupta, V. K., & Jiang, Y. (2018). New insights on bioactivities and biosynthesis of flavonoid glycosides. *Trends in Food Science & Technology, 79*, 116–124. https://doi.org/10.1016/j.tifs.2018.07.006

Yuan, Y., Tian, Y., Gao, S., Zhang, X., Gao, X., & He, J. (2023). Effects of environmental factors and fermentation on red raspberry anthocyanins stability. *LWT, 173*, Article 114252. https://doi.org/10.1016/j.lwt.2022.114252

Zang, Z., Tang, S., Li, Z., Chou, S., Shu, C., Chen, Y., Chen, W., Yang, S., Yang, Y., Tian, J., & Li, B. (2022). An updated review on the stability of anthocyanins regarding the interaction with food proteins and polysaccharides. *Comprehensive Reviews in Food Science and Food Safety, 21*(5), 4378–4401. https://doi.org/10.1111/1541-4337.13026

Zhang, S., Yu, Z., Sun, L., Ren, H., Zheng, X., Liang, S., & Qi, X. (2022a). An overview of the nutritional value, health properties, and future challenges of Chinese bayberry. *PeerJ, 10*, e13070.

Zhang, X., Jeffery, D. W., Li, D., Lan, Y., Zhao, X., & Duan, C. (2022b). Red wine coloration: A review of pigmented molecules, reactions, and applications. *Comprehensive Reviews in Food Science and Food Safety, 21*(5), 3834–3866. https://doi.org/10.1111/1541-4337.13010

Zhang, X., Lan, Y., Huang, Y., Zhao, X., & Duan, C. (2021). Targeted metabolomics of anthocyanin derivatives during prolonged wine aging: Evolution, color contribution and aging prediction. *Food Chemistry, 339*, Article 127795. https://doi.org/10.1016/j.foodchem.2020.127795

Zhang, Z., Li, J., & Fan, L. (2019). Evaluation of the composition of Chinese bayberry wine and its effects on the color changes during storage. *Food Chemistry, 276*, 451–457. https://doi.org/10.1016/j.foodchem.2018.10.054

Zhang, Z., Li, J., Fan, L., & Duan, Z. (2020). Effect of organic acid on cyanidin-3-O-glucoside oxidation mediated by iron in model Chinese bayberry wine. *Food Chemistry, 310*, Article 125980. https://doi.org/10.1016/j.foodchem.2019.125980

Zhao, Y.-W., Wang, C.-K., Huang, X.-Y., & Hu, D.-G. (2021). Anthocyanin stability and degradation in plants. *Plant Signaling & Behavior, 16*(12), 1987767. https://doi.org/10.1080/15592324.2021.1987767

Zhu, Y., Lv, J., Gu, Y., He, Y., Chen, J., Ye, X., & Zhou, Z. (2022). Mixed fermentation of Chinese bayberry pomace using yeast, lactic acid bacteria and acetic acid bacteria: Effects on color, phenolics and antioxidant ingredients. *LWT, 163*, Article 113503. https://doi.org/10.1016/j.lwt.2022.113503